Assessment of runoff sensitivities to changes in precipitation at the Indochina region

***Abstract*—Reliable assessment of runoff is a key for the prediction and management of freshwater resources. Therefore, hydroclimate forcing datasets, e.g., precipitation and total runoff (ROF) using the output from the multiple-realization, single-model ensemble named "d4PDF", were obtained in this study. Due to lack of direct observation of the ROF, we first evaluated the validity of the present-climate d4PDF precipitation using the Taylor diagram. The model was able to reproduce the extreme indices with a respectable performance regarding pattern correlations (0.6-0.9) and the centered-pattern RMSE (0.5-1). Finally, the runoff sensitivities, which are the relative change in ROF due to the change in various precipitation indices, were discussed. The results showed that the elasticity of runoff to precipitation is greater than unity for 83-95% of land grid cells during annual and wet-season time scale, indicated a faster response of the ROF under changing climate.**

Keywords—d4PDF; runoff generation; extreme indices

I. INTRODUCTION

It has been widely documented that warming of the climate will impact the hydrological cycle[1] with implications on the frequency and magnitude of water-related disasters at regional to continental spatial scales. In principle, analysis of the impacts of climate change on extreme events must be carried out before similar investigations of surface water. Analysis of extreme indices is a necessary first step for this kind of research[2]. Studies have unveiled significant changes in climate variables over the past century[3][4][5][6]. At the global scale, a tendency toward wetter conditions and more intense precipitation was observed at the majority of Earth's landmass throughout the 20th century based on an analysis of precipitation indices[5][6][7][8]. Analysis of hydroclimatic indices not only requires high-quality reference and model datasets, but also a sufficiently large amount of data. Global circulation models are a fundamental tool for climate change impact assessments despite their fundamental limitations and uncertainties, such as model uncertainty, emission scenarios, and internal variability[9][10]. Indochina (Fig. 1) is the continental region of Southeast Asia and is vulnerable to climate extremes due to its high population growth rate, low-lying geography, and exposure to tropical cyclones[11]. However, it lacks such analyses due to sparse data availability[12].

In this study, climatology indices calculated from the hydroclimate variables, e.g., precipitation and total runoff generation in Indochina, were analysed using a high-resolution, 60-km atmospheric general circulation model (AGCM) with 100-member simulations during 1951–2010 and 90-member simulations of future climate (2051–2110). Such large-ensemble, high-resolution models permit analysis of long-term trends and future changes in localised, severe events[13]. The simulation results are archived and freely available as the "Database for Policy Decision Making for Future Climate Change" (d4PDF). Subsequently, the d4PDF performance was evaluated using a gauge-based reference dataset, APHRODITE [14].

This study has two primary objectives: 1) performance evaluation of d4PDF in reproducing precipitation indices in the Indochina region, and 2) investigation of the relationship between precipitation and total runoff indices in terms of runoff elasticity under climate change conditions.

II. STUDY AREA

Indochina is the landmass area of southeast Asia, located around 91°E–109°25′E and 5°N–33°55′N. The region contains five countries: Myanmar, Thailand, Laos, Cambodia, and Vietnam. There are five major river basins constituting an area of 1,827,300 km^2 from Mekong (795,000 km^2), Irrawaddy (404,200 km^2), Salween (324,000 km^2), Chao Phraya (160,400 km^2), and Red (143,700 km^2). Climatologically, the region is affected by the Southeast Asian Monsoon system and interannual variability over the Pacific and Indian Oceans.

III. DATA

A. Daily reference precipitation

Daily "reference" precipitation data from 1951–2007 were obtained from APHRODITE, which is a continental-scale product containing a dense network of daily rain-gauge data for Asia, including the Himalayas, South and Southeast Asia, and the mountainous area of the Middle East. This product is based on data collected at 5,000–12,000 stations. In the V1101 product, an updated automatic quality control scheme was applied to remove error in gauge observations throughout the domain. Construction of a long-term daily gridded precipitation dataset was then carried out by interpolating the ratios of daily precipitation to daily climatology using a Sheremap-type scheme

B. Forcing datasets

The GCM outputs utilized in this study were generated by the atmospheric general circulation model MRI-AGCM 3.2H[15] developed at the Japan Meteorological Agency based on an operating numerical weather prediction model. Two sets of experiments performed using the AGCM were obtained: historical climate from 1951–2010 and +4K future simulations for 2051–2110. The present climate was simulated using a 100-member ensemble through perturbation of the initial and lower boundary conditions. The observed monthly-mean sea surface temperature (SST), sea ice concentration

(SIC), and climatological monthly sea ice thickness (SIT) are the lower boundary conditions of the AGCM model. For the +4 K simulation, in which the global mean surface air temperature is 4 K warmer than in the pre-industrial era and

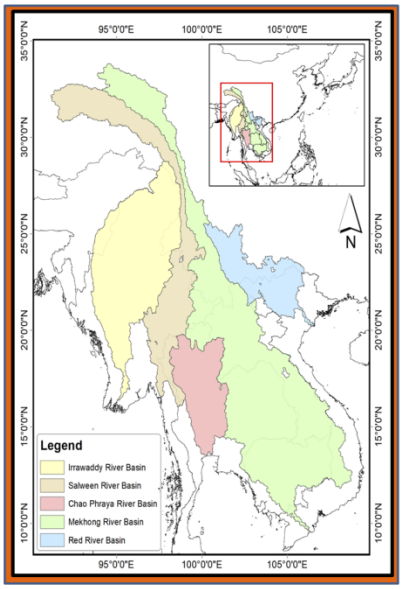

Fig. 1 Indochina region and its river basins

GHG levels are set to 2090 values from the RCP8.5 scenario, the climatological SST warming patterns (ΔSST) from six CMIP5 models were selected based on cluster analysis of the geographical patterns of SST changes. Each of the six ΔSSTs contains a 15-member ensemble, which result from small perturbations of the initial conditions and differing δSSTs, for a total of 90 members[13].

C. *Hydroclimate indices*

In this study, a total of 13 indices were used, of which six represented the core indices recommended by the Expert Team for Climate Change Detection Monitoring and Indices (http://etccdi.pacificclimate.org/). Seven additional indices, including number of days with more than 40 mm precipitation (R40), maximum 3-day precipitation amount (Rx3D), early monsoon cumulative precipitation amount (JJA), late-monsoon cumulative precipitation amount (SON), early dry-season precipitation amount (DJF), late dry-season precipitation amount (MAM), and total wet-season precipitation amount (Wet), were used in this study. Detailed information on each extreme index is given in Table I.

IV. METHODOLOGY

A. *Assessment of model performance*

Taylor[16] quantifies pattern similarity by using the correlation coefficient is a generic sense. Consider two variable f_n and r_n defined at N discrete spatial meshes. In this case, the correlation coefficient R between f and r is defined as

$$R = \frac{\frac{1}{N}\sum_{n=1}^{N}(f_n-\bar{f})(r_n-\bar{r})}{\sigma_f \sigma_r} \tag{1}$$

When f and r are the mean value of the d4PDF (model) and APHRODITE (reference) precipitation. σ_f and σ_r are the standard deviations of f and r, respectively. In order to isolate the differences in the patterns from the differences in the means of the two fields, the total RMSE (E) can be resolved into two components. First, the overall bias is defined as

$$\bar{E} = \bar{f} - \bar{r} \tag{2}$$

and the centered-pattern RMSE is defined by

$$E' = \left\{\frac{1}{N}\sum_{n=1}^{N}\left[(f_n-\bar{f})-(r_n-\bar{r})\right]^2\right\}^{1/2} \tag{3}$$

The center-pattern RMSE approaches zero when two patterns become more alike. All four of the above statistics (σ_f, σ_r, R, E') are useful in comparisons of patterns, and it is possible to display all of them in single diagram by recognize the relationship between these quantities of interest here,

$$E'^2 = \sigma_f^2 + \sigma_r^2 - 2\sigma_f\sigma_r R \tag{4}$$

B. *Elasticity of runoff to precipitation under climate change conditions*

Climate elasticity of runoff is an essential factor for quantifying the sensitivity of runoff to climate change, particularly at the catchment scale[17][18]. This study focused exclusively on the contribution of precipitation to the runoff elasticity in Indochina. Therefore, we adopted the framework provided by the study of Sankarasubramanian *et al*.[19], which applied in many previous studies, to estimate runoff elasticity using median descriptive statistics:

$$\varepsilon = median\left[\frac{(R_i-\bar{R})/\bar{R}}{(X_i-\bar{X})/\bar{X}}\right] \tag{5}$$

The value of the right term of Eq. (5) is calculated for each pair of R_i and X_i and the median of these values is the non-parametric estimator of climate elasticity of runoff.

Following Eq. (5), runoff elasticity to changes in precipitation can be estimated as

$$\epsilon_P(P,R) = median\left[\frac{(R_i-\bar{R})/\bar{R}}{(P_i-\bar{P})/\bar{P}}\right] \tag{6}$$

When R and P denote the 100-member means of runoff and precipitation extreme indices under the present climate (1951-2010). The value of the right-hand term in Eq. (6) is calculated for each pair of R_i and P_i between the seasonal and annual time series of present and future climate ensembles.

V. RESULTS

A. *Evaluation of the d4PDF ensemble reproduction of hydroclimate indices*

The d4PDF ensemble could reproduce climate indices in the Indochina peninsula, with correlation coefficients between 0.80–0.90 for seasonal (PRCPTOT, SON, and Wet), intensity

(R95p, Rx1D, Rx3D, and SDII), and frequency (R10) indices (Figure 2a). The reproduced dry-season indices, e.g., DJF and

Table I List of precipitation indices used in present study

ID	Units	Indicator name	Definitions
		Annual and seasonal precipitation indices	
PRCPTOT	mm	Annual total wet-day precipitation	Annual total PRCP in wet days (RR ≥ 1 mm)
JJA	mm	Early monsoon precipitation (June to August)	Cumulative PRCP during June to August
SON	mm	late monsoon precipitation (September to November)	Cumulative PRCP during September to November
Wet	mm	Total wet-season precipitation (June to November)	Cumulative PRCP during June to November
DJF	mm	Early dry-season precipitation (December to February)	Cumulative PRCP during December to February
MAM	mm	Late dry-season precipitation (March to May)	
		Intensity-based indices	
Rx1D	mm	Max 1-day precipitation amount	Annual maximum 1-day precipitation
Rx3D	mm	Max 3-day precipitation amount	Annual maximum 3-day precipitation
SDII	mm day^{-1}	Simple daily intensity index	Annual total precipitation divided by the number of wet days (defined as PRCP ≥ 1.0 mm) in the year
R95p	mm	Very wet days	Annual total PRCP when RR > 95^{th} percentile
		frequency-based indices	
R10	Day	Number of heavy precipitation days	Annual count of days when PRCP ≥ 10 mm
R20	Day	Number of very heavy precipitation days	Annual count of days when PRCP ≥ 20 mm
R40	Day	Number of days above 40 mm	Annual count of days when PRCP ≥ 40 mm

MAM, had larger spatial variabilities and biases than the others due to much higher normalized SD and lower correlation values (0.60-0.70). The Taylor diagrams revealed that d4PDF had a lower ability to depict country-scale intensity indices but maintained acceptable agreement with reference data in terms of seasonal (JJA, SON, DJF, PRCPTOT) and frequency indices (R10, R20, R40).

The outcomes for the Irrawaddy and Salween basins were comparable to the country-scale results (Figure 2b), with correlation coefficients of several indices of 0.40-0.80 and 0.60-0.85, respectively (Figures 2c and 2d). The results for the Mekong Basin (Figure 2e) exhibited equivalent characteristics to the former basins in terms of correlation (0.60–0.90) and normalised SD ratio (0.20–0.80), but a lower ability to reproduce the MAM, Rx1D, and DJF indices.

The Red River Basin showed spatial correlations of 0.60–0.85, wherein the correlations of the intensity indices were always higher than the seasonal and frequency indicators, except for R40 (Figure 2f). The simulated spatial variability was smaller than the reference precipitation in R10 and R20, with correlation coefficients of 0.40–0.63 and larger biases. The d4PDF exhibited the weakest ability to reproduce the SON and DJF indices for this basin.

Overall, there were broad discrepancies in the Rx1D biases among the d4PDF ensembles and the underperformance of dry-season indices (DJF, MAM) in basin-scale simulations, as shown in the diagram, suggesting that the indices were sensitive to perturbation of the initial conditions. However, the close grouping of dots representing the other indices (e.g., PRCPTOT, JJA, SON, SDII, R10, and R20) indicated that the simulated uncertainty at the spatial scale attributable to sampling variability was not very large.

B. Assessment of runoff sensitivity to changes in precipitation in the Indochina region

Based on the derived $\varepsilon_P(P,R)$ over Indochina, we determined the spatial distribution of runoff elasticities to changes in various extreme indices of P (Figure 3 and 4). The precipitation elasticities in the river basins had a spatial median ε_P for PRCPTOT and the wet-season indices (JJA, SON, and Wet) of 1.28–2.04. In 9.80–46.5% of the land grid cells, the relative P change was amplified by a factor of two or more into the relative R change. The results indicated that a 1% increase in the precipitation indices would result in an at least 1% increase in the associated runoff indices. The elasticity of R to changes in early dry-season climatology (DJF and MAM) were both positive, yet the median $\varepsilon_P(P,R)$ of DJF was slightly larger than unity (ε_p = 1.07), with 40.65% of land grid cells having $\varepsilon_P(P,R) > 1$. In many areas (e.g., central Irrawaddy, Lower Mekong, and Red Basins), higher median runoff sensitivities ranging from 2.2–4.8 were recorded during the early dry season in the future climate. By contrast, MAM climatology revealed a fairly different picture of the runoff response to ΔP with much higher median elasticity (ε = 1.95), accounting for a considerable portion of land grid cells where $0 < \varepsilon_P(P,R) \leq 5$ (75.62%), compared with 63.28% in DJF. The northern Irrawaddy and Lower Mekong Basins had the most consistent projections of runoff response, with $\varepsilon_P(P,R)$ from 7.2 to 12 for all future SSTs. The runoff elasticity to Rx1D

and Rx3D were lower than the seasonal indices, with median $\varepsilon_P(P,R)$ value of 0.81 and 0.71, respectively. The distribution of $\varepsilon_P(P,R)$ indicated that a given percentage change in P resulted in a greater percentage in R for the majority of land grid cells (38.77–42.70%).

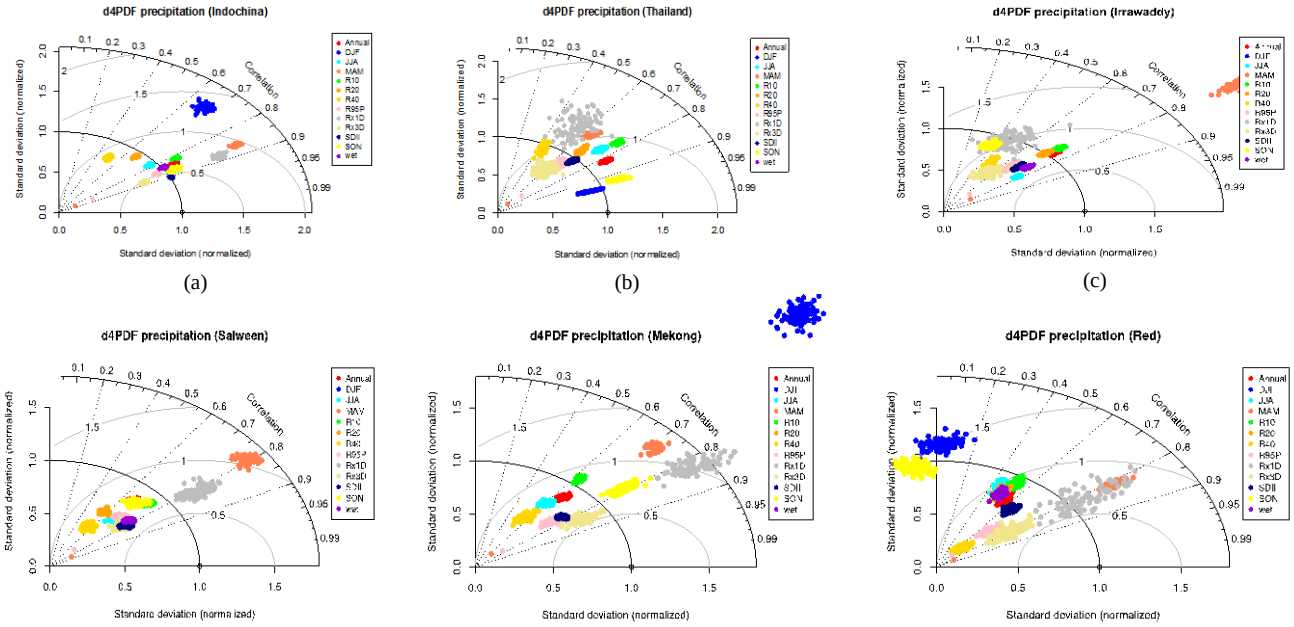

(a) (b) (c) (d) (e) (f)

Fig. 2 Taylor diagram (Taylor, 2001) comparing the abilities of the models to represent climate extreme indices over a) the Indochina region b) Thailand, c) the Irrawaddy Basin, d) the Salween Basin, e) the Mekong Basin, and f) the Red River Basin

The range of $\varepsilon_P(P,R)$ from the PRCPTOT from this study was comparable to but slightly lower than the results of Berghujis *et al.*[20], who showed that runoff elasticity to changes in annual mean precipitation had a median of 1.90 in a humid region, which includes Indochina, where the aridity index ($\phi = E_p/P$) ≤ 1.5. Moreover, the median elasticity of PRCPTOT was found consistent with the aforementioned study in the Lower Mekong under one of three future scenarios.

In the next section, we shall discuss the results and limitations of the findings related to the reproducibility of the d4PDF precipitation and runoff sensitivities from precipitation

VI. DISCUSSION

A. *Evaluation of model reproducibility and uncertainty of future projections*

Based on the overall results, we found using the Taylor's method that d4PDF performed well in simulating seasonal, intensity, and frequency-based indices despite some disagreements due to systemic biases in Rx1D at the basin scale.

These results, in particular those of R95p, are consistent with the findings of Kim *et al.*[21], who showed that models with mesoscale resolutions produced high fidelities in simulated extreme precipitation over Indochina, as shown by spatial correlations of 0.5-0.9 and centered-pattern RMSE of 0.5-1. Despite its versatility, a Taylor diagram can only express the terms of variance and correlation. In many cases, hydroclimatic variables exhibit nonlinear dependences, meaning they cannot be accurately determined using linear correlation. Therefore, Correa and Lindstrom[22] recently proposed the Mutual Information Diagram to address this issue by incorporating other types of relationships between the model and reference fields and highlighting those similarities and differences that are not identifiable via statistical quantities. Further issue of the diagram is the lack of an intrinsic mechanism to indicate uncertainty in either the observations or internal variability. In future investigations, we could expand the scope of model performance evaluation by adopting several approaches that could identify the predictability of climate models on an uncertainty basis and determine the robustness of predicted trend signals on seasonal to decadal timescales, such as relative entropy[23][24], the signal-to-noise ratio[25].

B. *Runoff elasticity under climate change conditions*

Eq. (5) was used to estimate the runoff elasticity to change in precipitation under climate change conditions because a vast amount of present-day ensemble data is available.

While the equation has been widely applied in previous studies[26][27], it is an approximate solution that omit the contribution to runoff elasticity from the other factors such as air temperature (T), net radiation (R_n), wind speed at a height of 2 m above the ground (U_2) and most importantly, evapotranspiration (E). Therefore, the simplification made in this study shows a fundamental limitation on the evaluation of runoff elasticity to changes in hydroclimate conditions.

The underlying assumption of Eq.5 is based on the Budyko framework, which has increasingly been used to quantify the relative elasticity of water resources to changes in aridity and other factors[28]. Such studies assume that R, E, and P follow the Budyko curve when aridity ($\phi = E_p/P$) changes, allowing the sensitivity of E and R to changes in ϕ and other factors (ω)

to be evaluated analytically. One of the inherent relationships between E and P in the form of water availability

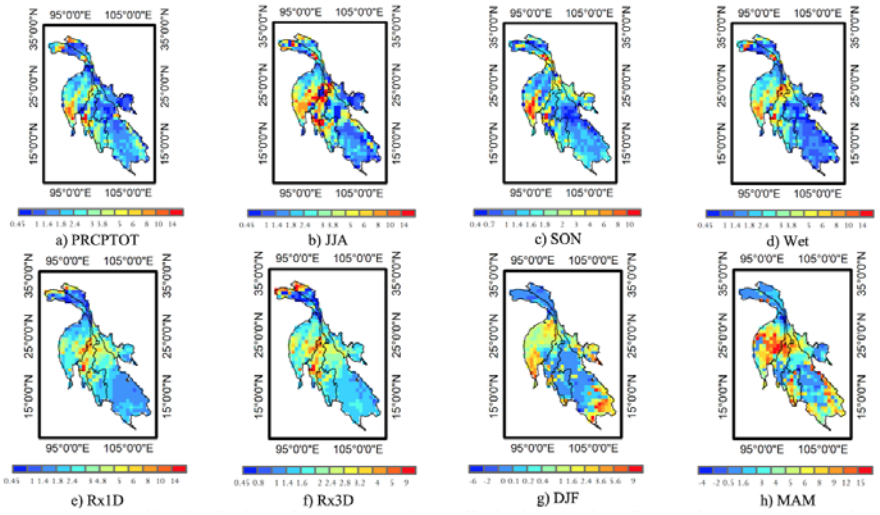

Fig. 3 Geographic distribution of SST-averaged runoff elasticity under climate change conditions for a) PRCPTOT, b) JJA, c) SON, d) Wet, e) Rx1D, f) Rx3D, g) DJF, and h) MAM

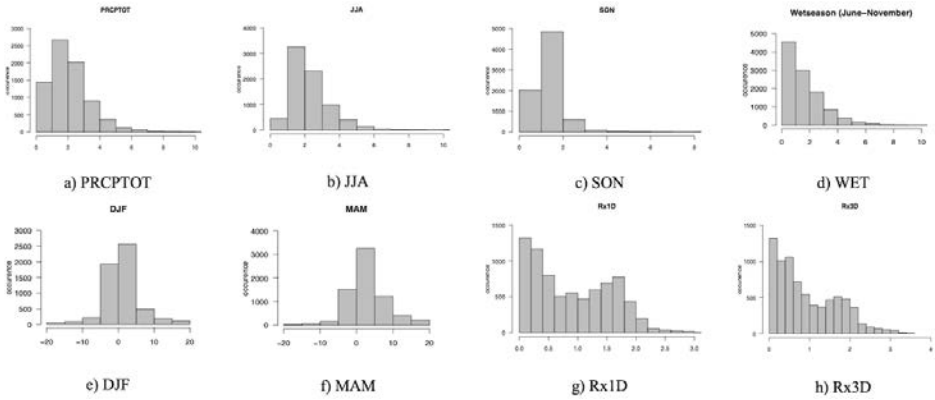

Fig. 4 Histogram showing the frequency distribution of the runoff elasticity from changes of the precipitation indices across the Indochina Region

($F(\phi,\omega) = E/P = 1\text{-}R/P$) was established by Fu[29] and considered very useful for quantifying the relative sensitivity of F to changes in ϕ and ω. However, the lumping of the sensitivity of R to P and E_p into a single term could lead to an underestimation of the contribution of ϕ changes. This might be a primary reason for the lower value of $\varepsilon_P(P,R)$ in the annual and intensity indices.

Future analysis on the runoff elasticity to changes in hydroclimate variables could be done using a revised approach to better attribute the effect of precipitation to changes in runoff and its relative contribution compared with E_p and ω, accounting for some uncertainty in the relevant parameters.

VII. CONCLUSION

This paper presents the analysis of runoff sensitivities to changes in precipitation at the Indochina Region by first checking the performance of d4PDF in reproducing precipitation indices, followed by the investigation of the relationship between precipitation and total runoff indices such as pattern correlation and runoff elasticity under changing climate. The model performed reasonably well in reproducing the reference precipitation characteristics in the present-day simulation, especially the wet-season climatology and intensity-based indices, with some basin-scale deficiencies detected in dry-season indices due to greater spatial variability and lower pattern correlations.

Finally, the sensitivities of runoff to changes in precipitation at the Indochina region was calculated using median estimation. The results showed that $\varepsilon_P(P,R)$ was always positive, with a median of 1.28–2.04 for the annual and seasonal indices and 0.71–0.81 for the Rx1D and Rx3D indices. Runoff elasticity was lower during the dry season, with 40.65–68.43% of the land grid cells having $\varepsilon_P(P,R) > 1$. The estimated annual runoff elasticity in this study was found lower than that of Berghujis *et al.*[20], which might represent inherent underrepresentation of precipitation in the non-parametric equation.

ACKNOWLEDGMENT

This study utilised the Database for Policy Decision-Making for Future Climate Change (d4PDF), and was produced using the Earth Simulator "Strategic Project with Special Support" of the Japan Agency for Marine–Earth

Science and Technology with cooperation among the Program for Risk Information on Climate Change, Social Implementation Program on Climate Change Adaptation Technology, Integrated Research Program for Advancing Climate Models, and Data Integration and Analysis System, which were all sponsored by the Ministry of Education, Culture, Sports, Science and Technology of Japan.

REFERENCES

[1] Hartmann, D.L., *et al.* 2013. Observations: Atmosphere and Surface. In: Climate Change 2013: The Physical Science Basis. The contribution of Working Group I to the Fifth Assessment Report of the Intergovernmental Panel on Climate Change [Stocker, T.F., Qin, D., Plattner, G.-K., Tignor, M., Allen, S.K., Boschung, J., Nauels, A., Xia, Y., Bex, V., and Midgley P.M. (eds.)]. Cambridge University Press, Cambridge, United Kingdom and New York, NY, USA.

[2] Sharma, D., and Babel, M.S. 2014. Trends in extreme rainfall and temperature indices in the western Thailand. *Int. J. Climatol.* **34**(7): 2393–2407.

[3] Frich, P., Alexander, L.V., Della-Marta, P., Gleason, B., Haylock, M., Klein Tank A.M.G., and Peterson, T. 2002. Observed coherent changes in climatic extremes during the second half of the twentieth century. *Clim. Res.*, **19**: 193–212.

[4] Peterson, T.C., Taylor, M.A., Demeritte, R., and Duncombe, D.L. 2002. Recent changes in climate extremes in the Caribbean region. *J. Geophys. Res.*, **107**(D21):4601. https://doi.org/10.1029/2002JD002251.

[5] Alexander, L.V., *et al*. 2006. Global observed changes in daily climate extremes of temperature and precipitation. *J. Geophys. Res.*, **111**: D05109, doi:10.1029/2005JD006290.

[6] Donat, M.G., *et al.* 2013. Updated analyses of temperature and precipitation extreme indices since the beginning of the twentieth century: The HadEX2 dataset. *J. Geophys. Res. Atmos.*, **118**: 2098–2118, doi:10.1002/ jgrd.50150.

[7] Chu, P.S., Chen, Y.R., and Schroeder, T.A. 2010. Changes in precipitation extremes in the Hawaiian Islands in a warming climate. *J. Clim.*, **23**: 4881–4900. https://doi.org/10.1175/2010JCLI3484.1.

[8] Niu, X., Wang, S., Tang, J., Lee, D.K., Gutowski, W., Dairaku, K., Mcgregor, J., Katzfey, J., Gao, X., Wu, J., Hong, S.Y., Wang, Y., Sasaki, H., and Fu, C. 2018. Ensemble evaluation and projection of climate extremes in China using RMIP models. *Int. J. Climatol.*, **38**: 2039–2055.

[9] Tebaldi, C., and Knutti, R. 2007. The use of the multimodel ensemble in probabilistic climate projections. *Philos. Trans. R. Soc.*, Ser. A, **365**(1857), 2053–2075.

[10] Hawkins, E., and Sutton, R. 2009. The potential to narrow uncertainty in regional climate predictions. *Bull. Am. Meteorol. Soc.*, **90**: 1095–1107. doi:10.1175/2009BAMS2607.1.

[11] Manton, M.J., *et al.* 2001. Trends in extreme daily rainfall and temperature in southeast Asia and the South Pacific: 1916-1998. *Int. J. Climatol.*, **21**: 269–284.

[12] Manton, M.J., and Nicholls, N. 1999. Monitoring trends in extreme climate events. Asia Pacific Network for Global Change Research, Tokyo. *APN Newsletter* **5**(1): 1–3.

[13] Mizuta, R., *et al*. 2017. Over 5000 years of ensemble future climate simulation by 60-km global and 20-km regional atmospheric models. *Bull. Am. Meteorol. Soc.* doi:10.1175/BAMS-D-16-0099.1.

[14] Yatagai, A. *et al.* 2012. APHRODITE: Constructing a long-term daily gridded precipitation dataset for Asia based on a dense network of rain gauges. *Bull. Am. Meteorol. Soc*. **93**: 1401–1415.

[15] Mizuta, R., Yoshimura, H., Murakami, H., Matsueda, M., Endo, H., Ose, T., Kamiguchi, K., Hosaka, M., Sugi, M., Yukimoto, S., Kusunoki, S., and Kitoh, A. 2012. Climate simulations using MRI-AGCM3.2 with the 20-km grid. *J. Meteor. Soc. Jpn.*, **90A**: 233–258.

[15] Taylor, K.E. 2001. Summarizing multiple aspects of model performance in a single diagram. *J. Geophys. Res. Atmos.*, **106**: 7183–7192.

[16] Schaake, J.C. 1990. From climate to flow, in *Climate Change and U.S. Water Resources*, edited by Waggoner, pp. 177–206, John Wiley, New York.

[17] Schaake, J.C. 1990. From climate to flow, in *Climate Change and U.S. Water Resources*, edited by Waggoner, pp. 177–206, John Wiley, New York.

[18] Yang, H., and D. Yang. 2011. Derivation of climate elasticity of runoff to assess the effects of climate change on annual runoff. *Water Resour. Res.*, **47**: W07526. https://doi:10.1029/2010WR009287.

[19] Sankarasubramanian, A., Vogel, R.M., and Limbrunner, J.F. 2001. Climate elasticity of streamflow in the United States. *Water Resour. Res.*, **37**(6): 1771–1781. doi:10.1029/2000WR900330.

[20] Berghuijs, W.R., Larsen, J.R., van Emmerik, T.H.M., and Woods, R.A. 2017. A global assessment of runoff sensitivity to changes in precipitation, potential evaporation, and other factors. *Water Resour. Res.*, **53**. https://doi.org/10.1002/2017WR021593.

[21] Kim, I.W., Oh, J., Woo, S., and Kripalani, R.H. 2018. Evaluation of precipitation extremes over the Asian domain: Observation and Modeling Studies. *Clim. Dynam.*, 1–26. https://doi.org/10.1007/s00382-018-4193-4.

[22] Correa, C.D., and Lindstrom, P. 2013. The mutual information diagram for uncertainty visualization. *Int. J. Uncertain. Quantif.*, **3**(3): 187–201.

[23] Kullback S. 1959. *Information Theory and Statistics*. John Wiley and Sons: New York.

[24] Shukla, J., Delsole, T., Fennessy, M., Kinter J., and Paolino, D. 2006. Climate model fidelity and projections of climate change. *Geophys. Res. Lett.*, **33**: L07702. doi: 10.1029/2005GL025579.

[25] Zwiers, F.W., and von Storch, H. 2004. On the role of statistics in climate research. *Int. J. Climatol*., **24**: 665–680

[26] Chiew, F.H.S. 2006. Estimation of rainfall elasticity of streamflow in Australia. *Hydrolog. Sci. J.*, **51**(4): 613–625.

[27] Novotny, E.V., and Stefan, H.G. 2007. Streamflow in Minnesota: indicator of climate change. *J. Hydrol.*, **334**(3–4): 319–333.

[28] Gudmundsson, L., Greve, P., and Seneviratne, S.I. 2016. The sensitivity of water availability to changes in the aridity index and other factors—A probabilistic analysis in the Budyko space. *Geophys. Res. Lett.*,**43**: 6985–6994. https://doi.org/10.1002/2016GL069763.

[29] Fu, B.P. 1981. On the calculation of the evaporation from land surface. *Sci. Atmos. Sin.*, **5**(1): 23–31 (in Chinese).